Electronic Supplementary Material (ESI) for RSC Advances

Electronic Supplementary Information

Highly Entangled Carbon Nanoflakes on $Li_3V_2(PO_4)_3$ Microrods for Improved Lithium Storage Performance

Linfeng Fei,[a] Wei Lu,[a] Li Sun,[a,b] Jiaping Wang,[b] Jiabing Wei,[c] Helen L. W. Chan,[a] and Yu Wang*[a]

[a] *Department of Applied Physics and Material Research Center, The Hong Kong Polytechnic University, Hong Kong SAR, P.R. China.*

[b] *Department of Physics and Tsinghua-Foxconn Nanotechnology Research Center, Tsinghua University, Beijing, P.R. China.*

[c] *Hefei Guoxuan High-tech Power Energy Co., LTD, Hefei, P.R. China.*

S1. Experimental details

Synthesis of $Li_3V_2(PO_4)_3$/C Composite: A facile ball-milling procedure followed by a solid-state carbothermal reduction reaction synthesis route was applied to prepare $Li_3V_2(PO_4)_3$ microrods/carbon nanoflakes composite. Typically, stoichiometric amounts of raw materials including $CH_3COOLi•2H_2O$ (15 mmol), NH_4VO_3 (10 mmol), $NH_4H_2PO_4•2H_2O$ (15 mmol), and sucrose ($C_{12}H_{22}O_{11}$, 17.5 mmol) were homogeneously mixed in ethanol (100 mL) by high-energy planetary ball-milling for 12 h then aged for another 12 h in tanks after operations. After being dried in an electronic oven at 80 °C for 24 h, the residual solid was grounded thoroughly before it was delivered to heating process. To form the $Li_3V_2(PO_4)_3$/C composite, the precursor was first heated (heating rate 5 °C/min) in a tube furnace at 450 °C for 2 h, followed by milling then heated at 850 °C for 12 h. The whole process was protected by a constant argon flow (see **Part S2**). After cooling (10 °C/min) to room temperature, the products were obtained by collecting the as-heated powder.

Structural Characterizations: Simultaneous thermogravimetric analysis & differential scanning calorimetry (TG-DSC) analysis was performed on a NETZSCH STA 449 C Jupiter® system under flowing argon/oxygen. X-ray diffraction (XRD) measurements were taken using a Rigaku SmartLab Intelligent X-ray Diffraction System with filtered Cu Kα radiation (λ = 1.5406 Å, operating at 45 kV and 200 mA). Rietveld refinement of XRD profiles were calculated by an integrated X-ray Powder Diffraction Software Package (PDXL Ver. 1.8.1.0, Rigaku). Raman measurements were taken using a Horiba Jobin Yvon LabRAM HR System with a laser wavelength of 514 nm. Scanning electron microscopy (SEM) observations were made on a JEOL 6335F system (operating at 10 kV). Transmission electron microscopy (TEM) images and energy dispersive X-ray spectrums (EDS) were obtained through JEM 2100F (field emission) transmission electron microscopes equipped with an Oxford INCA x-sight EDS Si(Li) detector at an acceleration voltage of 200 kV. Inductively coupled plasma-optical emission spectrometry (ICP-OES) was conducted on a PerkinElmer Optima 7300 V Spectrometers. The nitrogen adsorption and desorption isotherms at 77.3 K were obtained with a Micromeritics ASAP 2020 M+C Physisorption system. The tap density of the $Li_3V_2(PO_4)_3$/C composite was measured by placing 5 g of sample into a small glass vial

before tapping it by hand for 30 minutes until there was no visible volume reduction. The tap density was then determined from the tapped volume and its original mass.[1,2]

Electrochemical Measurements: Electrochemical performance measurements were taken using 2016 coin-type half-cells which were assembled in a glove box filled with protective argon gas (M. Braun inert gas systems Co. Ltd., Germany). The cathodes of the test cells were made from the active material, conductive Super P, and a poly(vinyl difluoride) binder in a weight ratio of 80 : 10 : 10. The cathode slurry was prepared by thoroughly mixing a N-methyl-2-pyrrolidine solution with the active material, Super P, and a poly(vinyl difluoride) binder. Consequently, the resulting slurry was deposited on aluminum foil (20 μm) and pressed before the entire assembly was dried in a vacuum oven at 120 °C overnight. Pure lithium foil was used as the anode, and a polypropylene separator (Celgard 2400) was used to separate the cathode and the anode. A 1 M $LiPF_6$ solution in ethylene carbonate (EC) and diethyl carbonate (DEC) mixed at a weight ratio of 1:1 was adopted as electrolyte in the test cells. The cyclic voltammetry performances were tested using a Potentiostat/Galvanostat (EG&G Princeton Applied Research 273A). The discharge and charge measurements were made on a Land battery test system (Wuhan Land Electronic Co., China) in a voltage window of 3-4.3 V at room temperature at different rates.

S2. Determination of heating conditions by TG-DSC

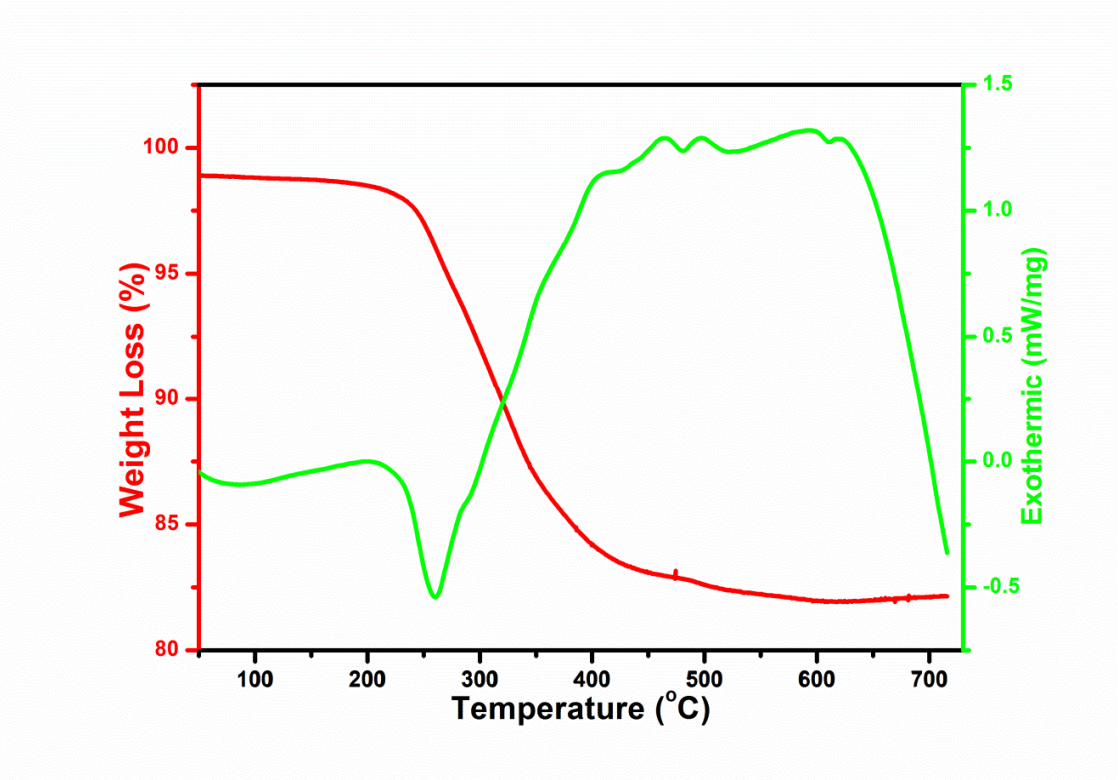

Figure S1. TG-DSC profiles of as-dried gel precursor under flowing argon.

TG-DSC profile of as-dried gel precursor under protective argon atmosphere is presented in **Figure S1**. A major weight loss segment accompanied by a clear endothermic process took place before 400 °C, suggesting the decomposition of various raw materials. The weight loss continued until about 750 °C together with a series of evident exothermic phenomena, implying the end of carbothermal reaction beyond 750 °C. In this case, a decomposition temperature of 450 °C and an annealing temperature of 850 °C were applied in our synthesis process to obtain well-crystallized $Li_3V_2(PO_4)_3$/C composite.

S3. Rietveld refinement of XRD profile

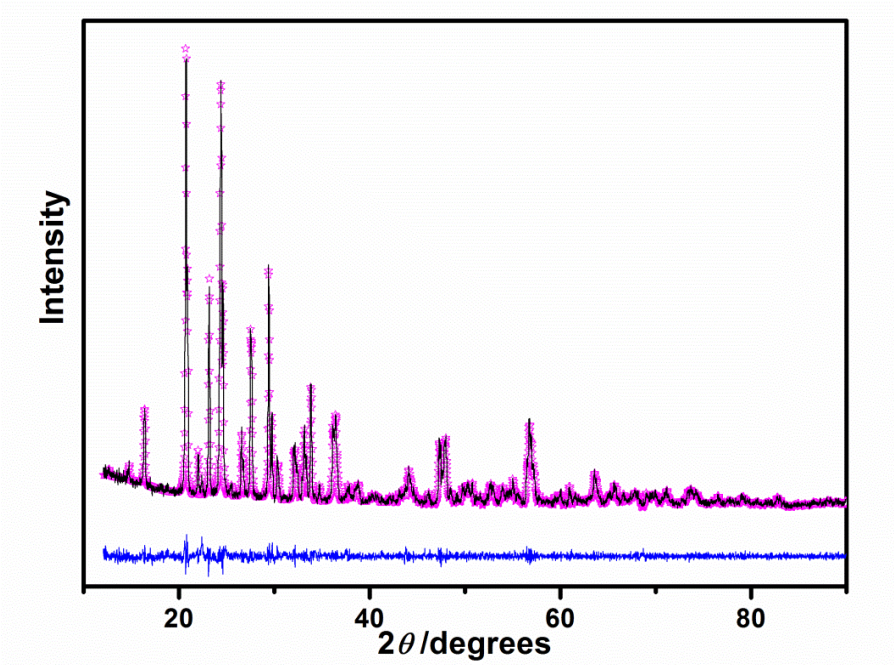

Figure S2. Rietveld refinement of XRD profile for $Li_3V_2(PO_4)_3$/C composite. The observed and calculated intensities were indicated by black line and purple stars, respectively. The bottom blue line represents the fitting residual difference.

Table S1. The lattice constants of $Li_3V_2(PO_4)_3$ calculated by a Whole Powder Pattern Fitting (WPPF) method.

a (ang.)	b (ang.)	c (ang.)	α (deg)	β (deg)	γ (deg)
8.6106(5)	8.5951(5)	12.0423(7)	90.000000	90.565(3)	90.000000

Table S2. Atomic sites and fractional coordinates of $Li_3V_2(PO_4)_3$/C:

Atom	x	y	z
Li1	0.202000	0.781000	0.182000
Li2	0.934000	0.312000	0.226000
Li3	0.576000	0.429000	0.207000
V1	0.251030	0.459350	0.109360
V2	0.753070	0.474510	0.390380
P1	0.106900	0.099600	0.158600
P2	0.607800	0.114900	0.355200
P3	0.039500	0.250900	0.488500
O1	0.927600	0.116300	0.146300
O2	0.148200	0.976900	0.240400
O3	0.172700	0.051600	0.034600
O4	0.161800	0.260900	0.184500
O5	0.422900	0.091200	0.326700
O6	0.695900	1.004500	0.284100
O7	0.641600	0.087600	0.477200
O8	0.643700	0.293300	0.314300
O9	0.950900	0.128400	0.569500
O10	0.930700	0.319400	0.402800
O11	0.172500	0.163000	0.431400
O12	0.105900	0.366200	0.576100

* The reliable factors are Rwp=9.22%, Rp=6.94%, and Re=7.77%.

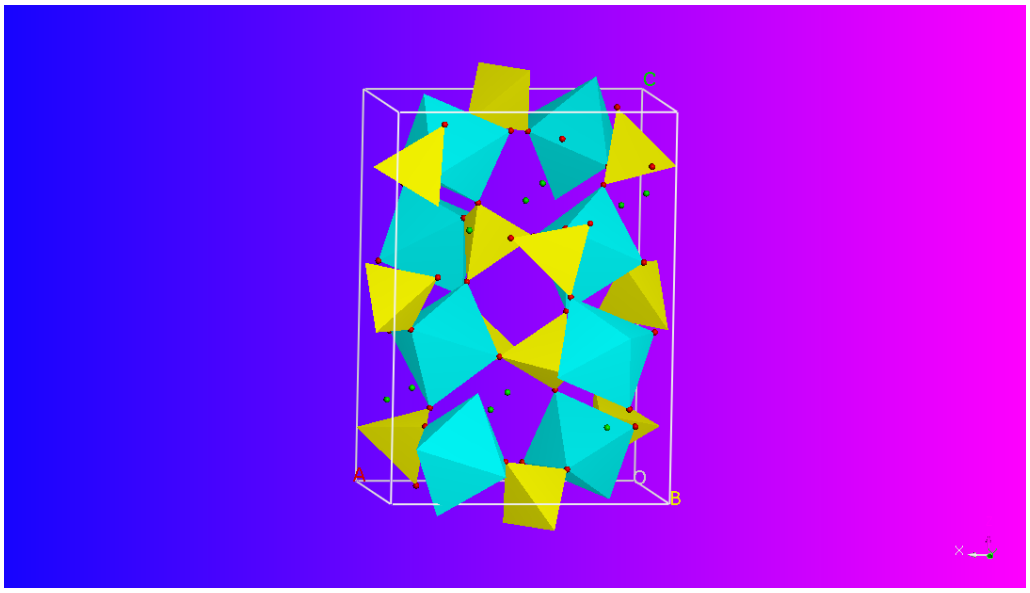

Figure S3. Sketch of the crystal structure of $Li_3V_2(PO_4)_3$ based on the refined data. Lithium atoms: green spheres; oxygen atoms: red spheres; phosphate tetrahedrons (PO_4): yellow blocks; and vanadium oxide octahedrons (VO_6): cyan blocks.

$Li_3V_2(PO_4)_3$ with a three-dimensional network consisting of slightly distorted metal octahedral and phosphorus tetrahedral linked together *via* common apical oxygen atoms, contains three independent lithium sites as shown by green spheres.[3,4] This unique arrangement enables three dimensional pathways for lithiation/delithiation, which is the reason why it is electrochemically better than $LiFePO_4$ which has just one dimensional pathway in the structure.[5] Yet the separate arrangement of transition metal cations (VO_6) by phosphate tetrahedrons (PO_4) results in relatively poor electrical conductivity.

S4. Reciprocal lattice calculations for SAED analysis

It is known that for a typical monoclinic lattice, the parameter relationship for the monoclinic cell should obey the following formula: $a \neq b \neq c$, $\alpha = \gamma = 90°$, $\beta \neq 90°$. Based on the as-refined crystallographic parameters, the interplaner spacing value for certain (h, k, l) can be calculated as:

$$\frac{1}{d^2} = \frac{h^2}{a^2\sin^2\beta} + \frac{k^2}{b^2} + \frac{l^2}{c^2\sin^2\beta} - \frac{2lh\cos\beta}{ac\sin^2\beta}$$

Moreover, the angle between the normal to two selected crystal planes (h_1, k_1, l_1) and (h_2, k_2, l_2) can be given by:

$$\cos\Phi = \frac{d_1 d_2}{\sin^2\beta}\left[\frac{h_1 h_2}{a^2} + \frac{k_1 k_2 \sin^2\beta}{b^2} + \frac{l_1 l_2}{c^2} - \frac{(l_1 h_2 + l_2 h_1)\cos\beta}{ac}\right]$$

In our case of $Li_3V_2(PO_4)_3$, the theoretical values of typical crystal planes are calculated and summarized in **Table S3**. These results were used in indexing repeatedly captured HRTEM/SAED images among many different crystallites, providing solid evidence that the as-obtained sample was indeed single-crystalline monoclinic $Li_3V_2(PO_4)_3$ microrods grown along the direction perpendicular to (001) plane.

Table S3. Typical reciprocal space parameters calculated from the refined structure.

u v w	h_1 k_1 l_1	h_2 k_2 l_2	R_2/R_1 ↑	Φ(deg)	D_1 (ang.)	D_2 (ang.)
0 0 1	-1 0 0	0 -1 0	1.002	90.00	8.610	8.595
1 1 1	-1 0 1	0 -1 1	1.006	70.44	7.037	6.996
1 1 2	-1 1 0	-1 -1 1	1.117	90.27	6.083	5.445
1 0 1	0 -1 0	1 0 -1	1.221	90.00	8.595	7.037
0 1 1	-1 0 0	0 -1 1	1.231	90.33	8.610	6.996
2 1 1	0 -1 1	1 -1 1	1.285	75.14	6.996	5.445
1 2 1	-1 0 1	1 -1 1	1.300	104.55	7.037	5.414
0 1 0	0 0 -1	-1 0 0	1.399	89.44	12.042	8.610
1 0 0	0 0 -1	0 1 0	1.401	90.00	12.042	8.595
2 0 1	0 -1 0	1 0 -2	1.734	90.00	8.595	4.957
2 1 2	-1 0 1	0 -2 1	1.739	78.83	7.037	4.048
0 2 1	-1 0 0	0 -1 2	1.746	90.46	8.610	4.931
1 1 0	0 0 -1	-1 1 0	1.980	89.60	12.042	6.083
1 0 2	0 -1 0	2 0 -1	2.114	90.00	8.595	4.067
0 1 2	-1 0 0	0 -2 1	2.127	90.19	8.610	4.048
1 2 0	0 0 -1	-2 1 0	3.128	89.49	12.042	3.849
2 1 0	0 0 -1	-1 2 0	3.132	89.75	12.042	3.845

* [*u v w*] is the zone axis; Φ is the angle between (h_1, k_1, l_1) and (h_2, k_2, l_2); D_1 and D_2 are the lattice distances of (h_1, k_1, l_1) and (h_2, k_2, l_2) in the real space.

S5. Determination of carbon content in the composite by TG-DSC

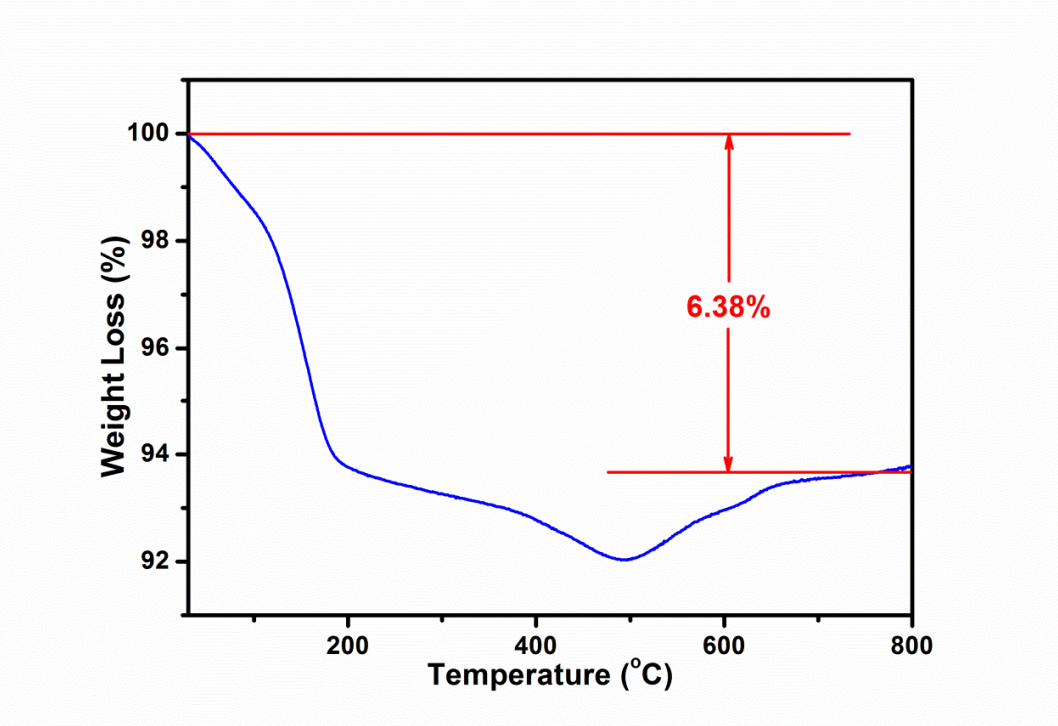

Figure S4. Thermogravimetric profile of the $Li_3V_2(PO_4)_3$/C composite heated in synthetic air.

Caculation of carbon content. In order to completely remove the carbon content, the $Li_3V_2(PO_4)_3$/C composite was heated in synthetic air flow within the temperature range from room temperature to 800 °C. Meanwhile, thermogravimetric analysis was recorded as shown in **Figure S4.** The weight loss is a result of the complete removal of carbon and oxidation of vanadium elements in the composite (from V^{3+} to V^{5+}). Thus the carbon content is estimated to be about 13.19% according to the reported method,[6] and is consistent with the ICP-OES result.

S6. First cycle CV profile of the $Li_3V_2(PO_4)_3$/C composite

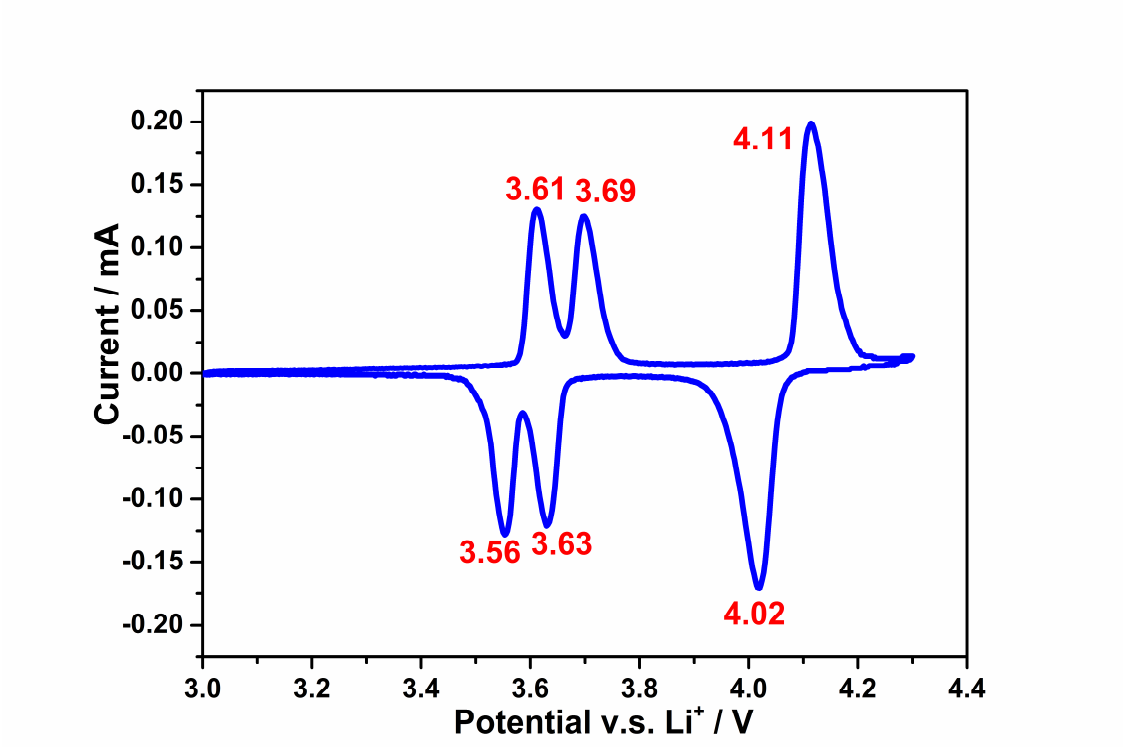

Figure S5. Cyclic voltammetry curve of synthesized $Li_3V_2(PO_4)_3$/C composite for the first cycle at a scan rate of 0.1 mV/s in the cell potential range of 3.0-4.3 V.

Cyclic voltammetry (CV) profile is recorded to gain understanding about the charge/discharge details of the as-fabricated cathode between 3.0 and 4.3 V at room temperature. As can be seen, three pairs of oxidation and reduction peaks appear in the first cycle. The first two anodic peaks at 3.61 and 3.69 V agreed with the removal of first Li^+ through two steps, corresponding to an ordered $Li_{2.5}V_2(PO_4)_3$ intermediate phase and a $Li_2V_2(PO_4)_3$ phase.[7,4] Then the second Li^+ was extracted by one step at 4.11 V to form $LiV_2(PO_4)_3$. The three cathodic peaks located at 3.56, 3.63, and 4.02 V are associated with the reinsertion of the two Li^+, resulting from the $V^{4+}/^{V3+}$ redox couple.

Bibliography

1. Z. Chen and J. R. Dahn, *Journal of The Electrochemical Society*, 2002, **149**, A1184–A1189.

2. M. Wang, Y. Yang, and Y. Zhang, *Nanoscale*, 2011, **3**, 4434–4439.

3. H. Huang, S.-C. Yin, T. Kerr, N. Taylor, and L. F. Nazar, *Advanced Materials*, 2002, **14**, 1525–1528.

4. S.-C. Yin, H. Grondey, P. Strobel, M. Anne, and L. F. Nazar, *Journal of the American Chemical Society*, 2003, **125**, 10402–10411.

5. J. Barker, R. K. B. Gover, P. Burns, and A. Bryan, *Journal of The Electrochemical Society*, 2007, **154**, A307–A313.

6. J. Chen and M. Whittingham, *Electrochemistry Communications*, 2006, **8**, 855–858.

7. H. Liu, P. Gao, J. Fang, and G. Yang, *Chemical Communications*, 2011, **47**, 9110–9112.